ELSEVIER

International Journal of Mass Spectrometry 214 (2002) 63–73

International Journal of Mass Spectrometry

www.elsevier.com/locate/ijms

Calibration of an audio-frequency ion trap mass spectrometer

Y. Cai [a,b], W.-P. Peng [a], S.-J. Kuo [a], H.-C. Chang [a,*]

[a] *Institute of Atomic and Molecular Sciences, Academia Sinica, P.O. Box 23-166, Taipei 106, Taiwan*
[b] *State Key Laboratory of Molecular Reaction Dynamics, Dalian Institute of Chemical Physics, Chinese Academy of Sciences, Dalian 116023, China*

Received 15 August 2001; accepted 31 October 2001

Abstract

A method for calibration of an audio-frequency (AF) ion trap mass spectrometer is described. The method is proposed to surmount the obstacle that there is a lack of a proper calibrant for mass spectrometers in the mass-to-charge ratio (m/z) range of 10^6 to 10^{10}. To calibrate such mass spectra, we determine the point of ejection, q_{eject}, on the stability diagram of the ion trap operated in a mass-selective axial instability mode. This is accomplished by measuring the radial secular frequencies (and therefore, the m/z value) of a single trapped particle using a light scattering method, followed by monitoring the action of particle ejection in real time to obtain the q_{eject}. A delayed ejection with $q_{\text{eject}} = 0.949 \pm 0.004$ is found at a trap driving frequency of $\Omega/2\pi = 200$–600 Hz. Theoretical analysis for the origin of the delayed ejection indicates that the delay is predominantly resulted from the existence of multipole components in the fields due to trap imperfections. Inclusion of -3% of the octopole with respect to the basic quadrupole field can satisfactorily account for our observations. An m/z accuracy approaching 0.1% is attainable after proper calibration of the AF ion trap mass spectrometer. (Int J Mass Spectrom 214 (2002) 63–73)

Keywords: Audio-frequency; Mass calibration; Single particle; Light scattering

1. Introduction

Since its invention by Paul and Steinwedel in 1960 [1], the quadrupole ion trap has been widely used as a device for spectral mass analysis of atomic, molecular and cluster ions [2,3]. In most of the commercial quadrupole ion trap mass spectrometer (QITMS) available to date, a radio-frequency (RF) ac field is applied between the ring and the end-cap electrodes of the trap in the frequency range of $\Omega/2\pi = 1$ MHz. This limits the mass analysis capability of such spectrometers to $<10^3$ for singly charged species [4,5]. Several techniques involving reduction of the radio frequency, trap size, along with the use of resonance ejection [5], have been implemented to extend the investigated mass/charge (m/z) range. However, the highest m/z value that has been reached at present is about 150,000 Da/charge [6]. Other methods like time-of-flight mass spectrometry and Fourier-transform ion cyclotron resonance mass spectrometry also suffer similar limitations [7–9]. This could be a misfortune since both mass and charge state determination of large particles (with $m/z > 10^6$) is often an important and necessary task in many fields of science.

In light of the importance of mass analysis of large bioparticles [8,9], we have recently developed an audio-frequency (AF) ion trap mass spectrometric

* Corresponding author. E-mail: hcchang@po.iams.sinica.edu.tw

1387-3806/02/$20.00
PII S1387-3806(01)00558-9

method to serve such purposes [10]. The method is rooted on the pioneering work of Wuerker et al. [11] who demonstrated the capability of trapping, detection and mass analysis of single microparticles using a quadrupole ion trap in 1959. Since then, the device has been frequently utilized as an electrodynamic balance for single aerosol analysis [12]. A mass accuracy of the order of 10^{-3} or better for particles weighing 10^{-16} kg can readily be attained [13–17]. The accuracy is comparable to that (0.1%) provided by the commercial RF QITMS [5], suggesting a possibility of utilizing this AF ion trap as a mass spectrometer. To obtain experimental data in a form of true mass spectrum, we adopted a standard mass-selective instability mode [4,5] by scanning the ac voltage applied between the ring electrode and the two trap end-caps. Employing this approach has allowed us to successfully extend the mass analysis range of the QITMS beyond 10^6 Da/charge [10].

One limitation in the mass/charge determination of particles in the domain $m/z > 10^6$ is the lack of a proper calibrant for the AF ion trap mass spectrometer whose performance may not exactly follow what the Mathieu's equations have predicted due to the existence of the gravitational force, buffer gas damping, and nonlinear fields in the trap. Hence, the point of ejection on the stability diagram (a_z vs. q_z) is likely to deviate significantly from $q_{\text{eject}} = 0.908$ at $a_z = 0$. In an earlier work [10], we calibrated the AF mass spectra by first utilizing the ion trap as an electrodynamic balance to determine the *m*/*z* value of a single particle and then detecting the particle ejection in real time. A value significantly larger than $q_{\text{eject}} = 0.908$ was determined, indicating a delay in particle ejection. We attribute the delay to imperfections of the ion trap used in the measurement and seek to examine in detail the origin of the delay in this work.

In a series of publications, Wang, Franzen and co-workers [18] provided a theoretical framework for the analysis of trapping and ejection properties of a nonideal (or nonlinear) ion trap. In all the cases that they considered, the strongest multipole field is the octopole. For a truncated quadrupole ion trap whose hyperbolic electrodes are cut to finite size, the octopole field has an opposite sign with respect to the basic quadrupole field. This results in delayed ejection of the trapped particles for the existence of a double well in the unstable region [19]. Wells et al. [20] have recently conducted both experiments and simulations to identify the mass shifts (or delays in ion ejection) caused by the holes on the end-cap electrodes for small molecules. They found that the end-cap holes can indeed lead to additional delays, which are compound-dependent due to collisions of the sample with background gas molecules.

We present in this article an analysis for the possible origin of the delayed ejection observed in our measurements using a homebuilt AF ion trap mass spectrometer. A direct comparison between calculations and measurements is attempted. In the following sections, after a brief description of the experiments conducted to acquire the mass spectra of single submicron-sized particles, a theoretical treatment for the origin of the experimentally detected ejection delay is provided.

2. Experiments and results

2.1. Experimental setup

Details of the experimental setup have been described in [10] and, therefore, only a brief description is given here. Fig. 1 depicts a schematic diagram of the setup, which mainly consists of an electrospray ionization (ESI) source, a quadrupole ion trap (QIT), and a scattered laser light detection system. The ESI source comprises a needle (200 μm in diameter) and an entrance plate with an orifice diameter of 150 μm. A 4 kV dc is applied between the needle and the plate to create a positively charged spray. The trap has an unstretched geometry of $z_0 = 7.07$ mm and $r_0 = 10$ mm, essentially identical to that of the ion trap detector used by Louris et al. [4]. On this device, two holes (3.1 mm in diameter) are drilled in the two end-caps to provide pathways for particle injection and ejection, while the four holes (3.8 mm in diameter) on the ring electrode are made to allow illumination and visualization of the particles inside the ion trap. Applied to

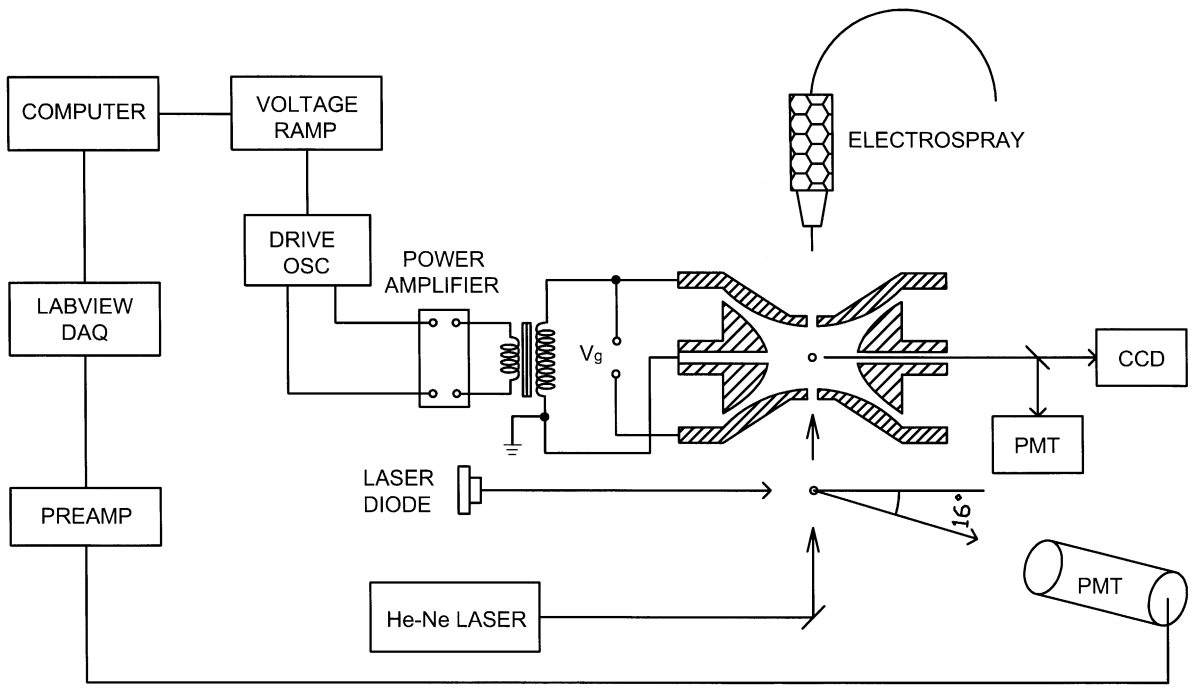

Fig. 1. Schematic diagram of the experimental setup. Note that two separate detection schemes are used to probe the individual particles inside and outside the quadrupole ion trap simultaneously.

the end-caps is a frequency-variable ac voltage from a high-voltage transformer driven by an AF power amplifier. The ring electrode is kept at ground potential and so one can float the two end-caps at a small dc voltage (V_g) to balance the gravitational force (Fig. 1).

To acquire the mass spectra using this AF ion trap, a standard mass-selective instability mode [3] is adopted. The method is combined with a light detection scheme to identify charged particles ejected from the trap on a single particle basis. Before the particle ejection, the chamber is backfilled with 1 mTorr He buffer gas to retain the particle in the trap center and, at the same time, reduce both the axial and the radial amplitudes of the particle's oscillatory motions. The ac voltage amplitude (V_{ac}) is ramped from 420 to 1700 V (with $V_g = 0$) during the course of the particle ejection to obtain a full scan of the spectrum. In conducting this experiment, a 50 mW laser diode is employed as the illuminator, providing a power density of $\sim$10 kW/m^2 at the point of light scattering. A photomultiplier tube (PMT), situated at a forward scattering angle of 16°, detects the light pulses produced by the ejected particles as they pass through the illuminating laser beam.

2.2. Characterization of the quadrupole ion trap

To characterize the AF ion trap, primarily its stability diagram, we determined the secular frequencies of a single particle moving inside the trap using the method of Schlemmer et al. [17]. A 10 mW He–Ne laser illuminates the particle from the lower end-cap of the ion trap and the resulting scattered laser light is collected by a PMT through one hole on the ring electrode (cf. Fig. 1). Fourier-transform of the PMT signals collected in real time yields the secular frequencies of the trapped particle. Fig. 2 displays the result of a typical measurement with the time-domain data acquired in 30 s for the radial secular frequency (ω_r) of a single diamond microparticle (roughly

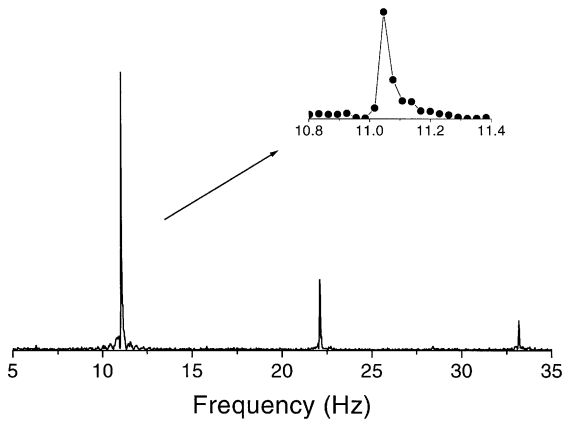

Fig. 2. Fourier-transform spectrum of the particle motions in the radial direction. In this example, the secular frequency is determined to be $\omega_r/2\pi = 11.050 \pm 0.015$ Hz and its harmonics can also be detected at $2\omega_r$ and $3\omega_r$ in the same spectrum. Data of this spectrum were acquired in a 30 s measurement.

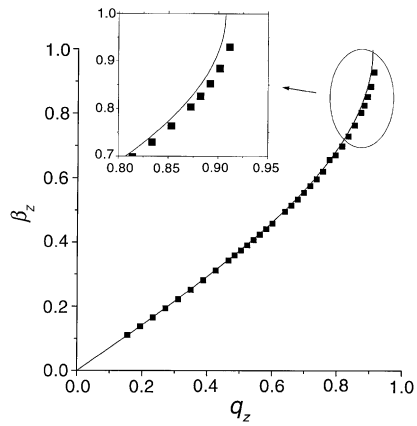

Fig. 3. Experimentally determined stability diagram (β_z vs. q_z) along the $a_z = 0$ axis of the ion trap used in the present experiment. The solid curve represents the theoretically calculated result for an ideal quadrupole ion trap.

1 μm in diameter). As seen, an accuracy of the order of $\Delta\omega_r/\omega_r = 10^{-3}$ can be readily obtained from repeated measurements of the frequency in 3 min.

For an ideal quadrupole ion trap, the analysis based on a pseudopotential model [2,3] yields

$$\omega_r = \frac{V_{\mathrm{ac}}}{\sqrt{2}(m/z)r_0^2\Omega}, \tag{1}$$

$$\beta_z = \frac{2\omega_z}{\Omega} = \frac{4\omega_r}{\Omega}, \tag{2}$$

where $r_0^2 = 2z_0^2$, and ω_z and ω_r are the axial and the radial secular frequencies of the particle motions, respectively. Eqs. (1) and (2) hold only at $q_z \leq 0.4$, with the trap parameter defined by

$$q_z = \frac{4V_{\mathrm{ac}}}{(m/z)r_0^2\Omega^2} \tag{3}$$

Accordingly, the mass-to-charge ratio of the particle can be determined from its radial secular frequency by $m/z = V_{\mathrm{ac}}/\sqrt{2}r_0^2\Omega\omega_r$ at smaller V_{ac}.[1] At $q_z > 0.4$, a more complicated set of equations should be applied [2,3].

[1] The frequency shift due to the presence of the gravitational force and the applied dc field is too smaller [27] to change the presently measured delay in particle ejection.

Fig. 3 depicts a plot of β_z vs. q_z, obtained from the experimentally measured data ω_r at the fixed frequency $\Omega/2\pi = 300$ Hz and various ac voltage amplitudes V_{ac}. The result, in general, agrees well with the theoretical prediction for an ideal ion trap (denoted by the solid curve). However, significant deviation between experiment and theory emerges at $q_z > 0.5$ and, furthermore, the deviation becomes much more prominent at a larger q_z, as shown in the inset in Fig. 3. It should be noted that in this measurement, the highest point that can be reached is $\beta_z = 0.911$. The data beyond this point are unavailable since the amplitude of the particle motion in the axial direction at $\beta_z > 0.911$ is too large to allow precise measurement of ω_r. To assess the point of the particle ejection, we varied the V_{ac} slowly and observed directly the variation of particle motions inside the trap using the CCD camera (Fig. 1). From the action of the particle ejection, we determined $q_{\mathrm{eject}} \approx 0.935$. The value significantly deviates from 0.908, a clear indication that the ion trap used in the present experiment is not perfect. The device behaves like an ideal three-dimensional quadrupole ion trap (within the limit of our experimental detection sensitivity) only when functioning at $q_z < 0.5$.

2.3. Determination of ejection delay

The $q_{\text{eject}} = 0.935$ attained above is the value determined under a stationary condition, namely, the ac voltage amplitude is scanned infinitely slowly and the gravitational force is properly balanced by applying a small dc voltage (typically $V_g = 10$ V) across the two end-cap electrodes (see footnote 1). It forecasts a delay in particle ejection to occur due to the trap imperfections. Additional ejection delays, arising from the use of a non-zero scan rate of V_{ac}, are expected to appear in practical measurements. Such delays, as have been discussed before [5,21], can be rather severe for a trap operating in the AF region if the ac voltage is ramped too rapidly.

In this experiment, a scan rate of 100 V/s is adopted for V_{ac} to minimize the ejection delay and, simultaneously, maintain a good mass/charge resolution. A combination of Eqs. (1)–(3) yields

$$q_{\text{eject}} = \frac{V_{\text{eject}}}{V_{\text{fm}}} \frac{4\sqrt{2}\omega_r}{\Omega} \tag{4}$$

where V_{fm} and V_{eject} are the ac voltage amplitudes at the points of frequency measurement ($q_z < 0.4$) and particle ejection, respectively. The equation reveals that one can determine the q_{eject} simply by knowing the amplitude ratio $V_{\text{fm}}/V_{\text{eject}}$, rather than on their absolute values. This allows fairly accurate determination of q_{eject}. From a series of measurements, we determined an ejection point to locate at 0.949 ± 0.004, which varies only slightly (within the limit of our experimental uncertainty) with $\Omega/2\pi$ over the frequency range of 200–600 Hz. Compared to 0.935 obtained earlier, the value evidences the presence of an additional delay in particle ejection due to the finite scanning rate of V_{ac} ($\Delta V_{ac}/\Delta t = 100$ V/s) used in the present measurement.

2.4. Single-particle mass spectrum

To provide an overview for the performance of the AF ion trap mass spectrometer, a typical mass spectrum of amino-polystyrene microspheres is depicted in Fig. 4. The spheres, having a mean diameter of $0.91 \pm 0.022\,\mu$m and surface-functionalized with aminoheptyl groups [$-(CH_2)_7NH_2$], serve as an ideal test sample for this spectrometer. As described in detail elsewhere [10], we introduced the particles into the ion trap through a beam tube using an electrospray ionization source (Fig. 1). The ion source is operated in a positively sprayed mode and, hence, the particles are conceivably charged with protons and fully isolated in the gas phase. A suspension containing 0.5% (w/v) amino-polystyrene particles in 80:20 CH_3OH/H_2O solution at pH = 3.9 is typically used as the spray solution. The concentration of the suspension is kept low to ensure that there exists at most one single polystyrene microsphere in each spray droplet.

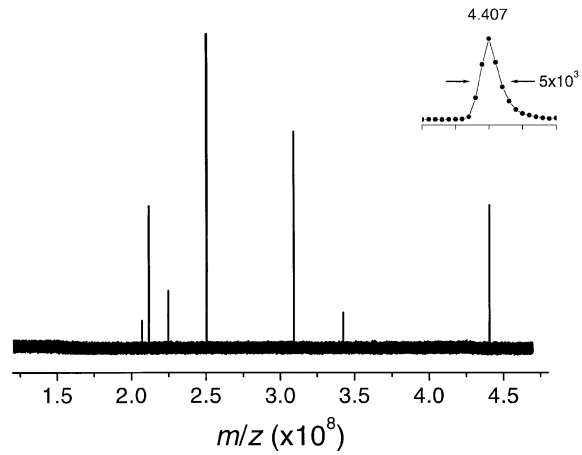

Fig. 4. Single-particle mass spectrum of monodisperse polystyrene microspheres. Inset: enlarged view of a typical scattered laser light pulse with a full width at half maximum of $\Delta(m/z) = 5 \times 10^3$, suggesting a mass resolution exceeding 10^4 for this single-particle mass spectrometer.

Fig. 4 depicts a spectrum acquired with use of the AF trap operating at $\Omega/2\pi = 600$ Hz and V_{ac} varying from 420 to 1700 V. The spectrum exhibits a nearly random distribution of the peak heights of the scattered laser light pulses. Only about 10 particles are being trapped and analyzed in this measurement, as viewed directly from the CCD camera (Fig. 1). In analogy to detection of single molecules in condensed phase [22], the difference in peak height between different particles in the spectrum is derived from the Gaussian

profile of the laser beam since not all the ejected particles traverse through the beam at the same spot and, hence, experience the same illumination intensity. The analogy, together with the low particle density, strongly corroborates the suggestion that the individual peak in Fig. 4 is derived from one single particle [10]. Namely, the figure exhibits a single-particle mass spectrum.

3. Simulations and results

3.1. The Mathieu equations

The equation of motion of a particle under the influence of gravitation and aerodynamic drag in an ideal quadrupole ion trap has a form in the axial direction [23,24],

$$\frac{\mathrm{d}^2 z}{\mathrm{d}\xi^2} + b\frac{\mathrm{d}z}{\mathrm{d}\xi} + (a_z - 2q_z\cos 2\xi)z = \frac{4F_\mathrm{g}}{m\Omega^2}, \tag{5}$$

where $\xi = \Omega t/2$, and F_g is the gravitational force. The damping term $b\,\mathrm{d}z/\mathrm{d}\xi$ is included here on the premise that the aerodynamic drag force (F_d) is in linear proportion to the velocity of the particle, namely, statistical fluctuation is ignored. Dahneke [25] has provided a full analysis to evaluate the F_d from the viewpoint of inelastic collisions between gas molecules and a single particle (either spherical or nonspherical) in the free molecular flow region. For a sphere with a diameter much larger than the mean free path of background gas molecules in thermal equilibrium, the damping force can be expressed in terms of

$$F_\mathrm{d} = -\frac{(8+\pi f)}{4}\frac{pm\upsilon}{\rho_0 d}\sqrt{\frac{8M}{\pi RT}}, \tag{6}$$

where $f \approx 0.9$ is the fraction of molecules reflected in a diffuse manner, p is the buffer gas pressure, M and T are the molar weight and temperature of the buffer gas molecules, and υ, ρ_0 and d are the velocity, density and diameter of the investigated particle, respectively. This alternately suggests a damping constant

$$b = \frac{8.6p}{\rho_0 d\Omega}\sqrt{\frac{M}{RT}}. \tag{7}$$

Given with the parameters $d = 0.91\,\mu\mathrm{m}$, $\rho_0 = 1.05\,\mathrm{g/cm^3}$, $p = 1\times10^{-3}\,\mathrm{Torr}$, $M = 4\,\mathrm{g/mol}$, $T = 300\,\mathrm{K}$, and $\Omega/2\pi = 300\,\mathrm{Hz}$, a unitless number $b \approx 0.001$ is reached. The value is about four times greater than that of Hars and Tass [16], who ignored the large size difference between the submicron-sized particle and the buffer gas molecules in their analysis.

One may assess how the axial secular frequency of the particle is altered due to the presence of buffer gas. The magnitude of the shift is estimated from the solution for a damped oscillator [15],

$$z = A_z\,\mathrm{e}^{-kt}\cos(\omega_z t), \tag{8}$$

where $\omega_z = \sqrt{(\omega_{0z}^2 - k^2)}$ and $k = b\Omega/4$. In the case of damping by He atoms with a constant of $b = 0.001$, the relative frequency shift caused by the aerodynamic drag is $(k/\omega_z)^2 \approx 10^{-5}$ for $\omega_z \approx \Omega/10$ and $\Omega/2\pi = 300\,\mathrm{Hz}$. The shift is much smaller than our experimental uncertainty ($\sim10^{-3}$) and, hence, can be neglected in the present analysis.

Fig. 5 displays the result of a computer simulation for the oscillation of a single particle trapped within

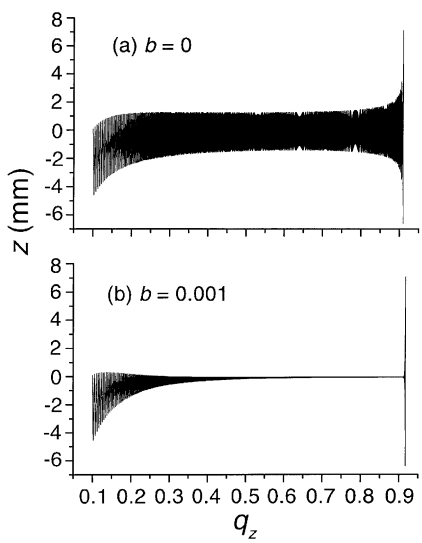

Fig. 5. Variations of the particle position z with the trap parameter q_z for a single particle confined within an ideal quadrupole ion trap without (a) and with (b) buffer gas. Due to the gravity, the particle is situated below the central plane of the trap. Note that in the simulation, the ac voltage amplitude is ramped at a rate of 100 V/s as used in the present experiment.

a pure quadrupole field using Eq. (5) and the parameters $a_z = 0$, $g = 9.81\,\mathrm{m/s^2}$, $\Omega/2\pi = 300\,\mathrm{Hz}$, and $\Delta V_{ac}/\Delta t = 100\,\mathrm{V/s}$. In this simulation, the q_z value is varied over the range, 0.10–0.95, for two cases ($b = 0$ and 0.001). As illustrated in Fig. 5a for a collision-free system ($b = 0$), the gravitational force exerts its influence by shifting the particle position below the trap center. The average shift decreases gradually with q_z and eventually converges to $\langle z \rangle \approx 4g/\Omega^2 = 11\,\mu\mathrm{m}$ as q_z approaches 0.908 [15]. At $q_z = 0.908$, where the gravitational effect is minimal, the particle motion becomes unstable and the oscillation amplitude enlarges exponentially with time. As soon as the amplitude is larger than $z = 7.07\,\mathrm{mm}$, the particle is ejected out of the ion trap. Note that in this simulation, a small ejection delay is resulted, $q_{\mathrm{eject}} = 0.914$, due to the finite scan rate of the ac voltage ($\Delta V_{ac}/\Delta t = 100\,\mathrm{V/s}$). All the simulated q_{eject} values, however, are insensitive to Ω, as shown in Fig. 6a for an ideal quadrupole ion trap.

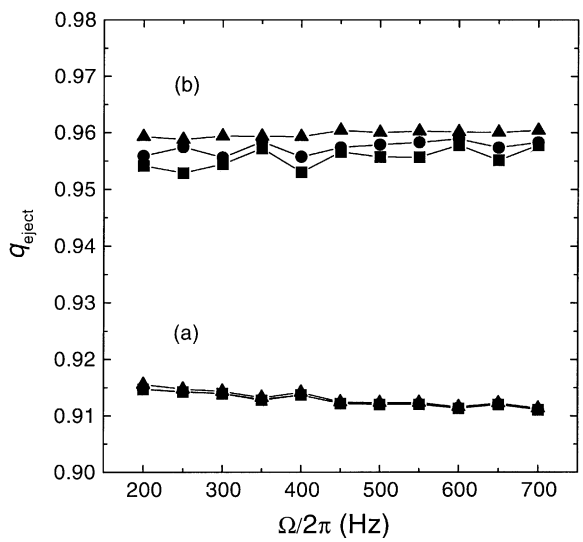

Fig. 6. Dependence of the ejection point (q_{eject}) on the trap driving frequency (Ω) in the cases of (a) $A_4/A_2 = 0\%$ and (b) $A_4/A_2 = -3\%$. The data points, denoted by (■), (●), and (▲), are results obtained with the damping constant of $b = 0$, 0.001, and 0.005, respectively.

3.2. Ejection delay due to ion trap imperfections

The value $q_{\mathrm{eject}} = 0.935$ determined in the prior section provides the first experimental evidence that the trap used in this work is nonlinear. One may attribute this non-linearity to the trap imperfections, which include truncation of the hyperbolic electrodes, drilling of holes on the electrode assemblies, machining inaccuracy, as well as any possible misalignments of the ring electrode with respect to the two end-caps. These imperfections are subject to further theoretical analysis.

Following Wang and co-workers [18], we introduce an octopole term to the modified Mathieu equation (Eq. (5)) to describe the particle motion in our trap with a cylindrical symmetry as

$$\Phi(\rho,\theta,t) = \Phi_0(t)\left[A_2\left(\frac{\rho}{r_0}\right)^2 P_2(\cos\theta) + A_4\left(\frac{\rho}{r_0}\right)^4 P_4(\cos\theta)\right], \quad (9)$$

where $\Phi_0(t) = -V_{ac}\cos(\Omega t)$ and $P_n(\cos\theta)$ is the Legendre polynomial of the order n ($n = 2$ and 4 in the present case). The strength of the octopole field is given here as a percentage of this component with respect to the strength of the quadrupole field, i.e. $(A_4/A_2) \times 100$. As pointed out by the authors [18], superposition of this field with the existing quadrupole can result in a change in both the secular frequency and the point of ion ejection [18–20]. To provide a more quantitative measure, we estimate this percentage by calculating the q_{eject} and fitting it to the experimentally determined value. It is calculated from the modified equation of motion that use of the octopole field with a magnitude of $A_4/A_2 = -3\%$ can properly reproduce the experimental data, $q_{\mathrm{eject}} = 0.935$ at $\Omega/2\pi = 300\,\mathrm{Hz}$.

One may explore further the additional ejection delays caused by the non-zero V_{ac} scan rate coupled with the field distortion ($A_4 \neq 0$). Fig. 7(a–e) display the results of computer simulations for the variation of the particle position (z) with time as q_z is scanned from 0.90 to 0.99 at various values of A_4/A_2. As shown, a

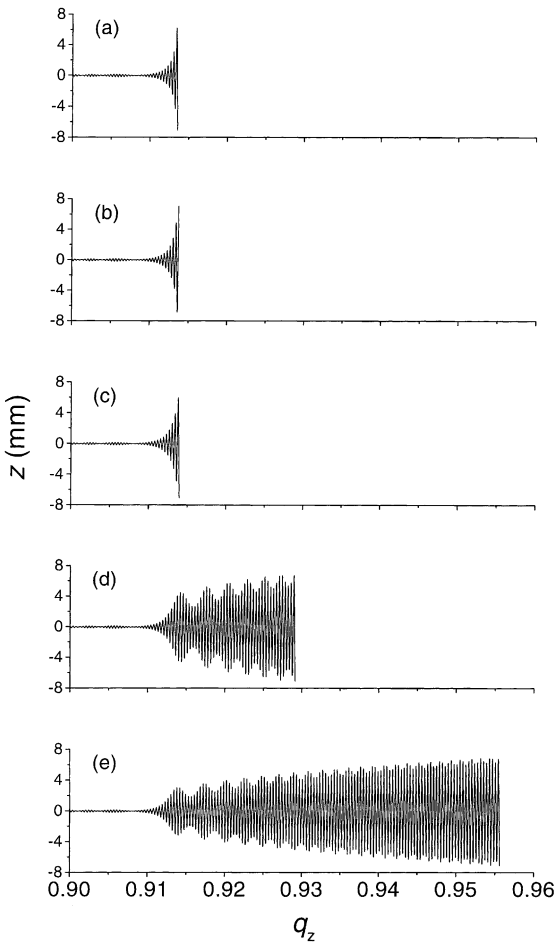

Fig. 7. Variations of the particle position z with the trap parameter q_z for a single particle confined within a nonlinear ion trap. The parameters used in the simulations are $b = 0.001$, $\Delta V_{ac}/\Delta t = 100$ V/s, $z(0) = 0.1$ mm, $\dot{z}(0) = 0$ mm/s, and (a) $A_4/A_2 = +3.0\%$, (b) $A_4/A_2 = +1.5\%$, (c) $A_4/A_2 = 0$, (d) $A_4/A_2 = -1.5\%$, (e) $A_4/A_2 = -3.0\%$, respectively.

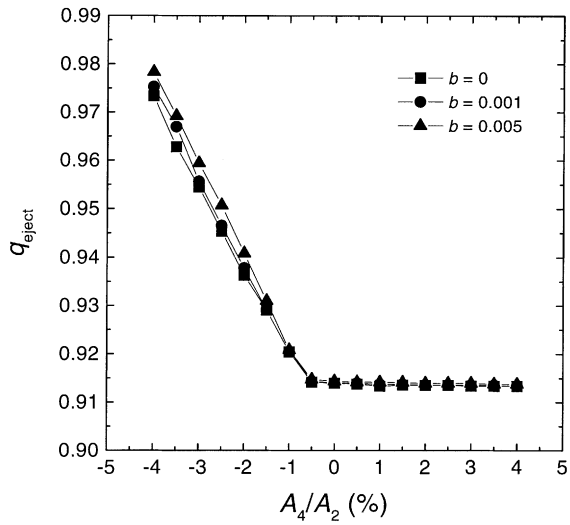

Fig. 8. Dependence of the ejection point (q_{eject}) on the percentage (A_4/A_2) of the octopole field with respect to the basic quadrupole field in the ion trap. The data points, denoted by (■), (●), and (▲), are results obtained with the damping constant of $b = 0$, 0.001, and 0.005, respectively.

field with a positive octopole component can cause a slightly earlier particle ejection [18], while inclusion of a negative octopole term in the field induces an obvious delay in ejection. Consequently, the former has an effect of enhancing mass resolution [18], whereas the latter degrades it due to the much slower ejection rate for the particle. The behavior is highly asymmetric, with a more prominent effect appearing on the negative side of A_4/A_2 (cf. both Figs. 7 and 8).

In Fig. 6, we also compare in parallel the results of $A_4/A_2 = 0$ and -3% at $\Omega/2\pi = 200$–700 Hz. A larger variation in q_{eject} is noticeable among cases of various b for the nonlinear ion trap (Fig. 6b). It conveys an important message that extension of the ejection delay by the buffer gas can occur more easily in this case. From a direct comparison of our measurements with the calculations depicted in Fig. 6, we found that one can properly reproduce the experimental value ($q_{eject} = 0.949 \pm 0.004$) when -3% of the octopole component is included in the calculation ($q_{eject} \approx 0.957 \pm 0.002$). The result is in close agreement with the conclusion reached earlier, demonstrating the consistency of the present measurements. [2]

We emphasize that the good match of the results between experiment and simulation reported herein for a field containing -3% octopole might be purely

[2] In an earlier work, we determined that the velocity of the particles ejected from the ion trap is about 20 m/s [10]. With this velocity, it will take only about 0.5 ms for the particle after ejection to reach the detection region. The flight time is too short to create any noticeable delay in our observation.

fortuitous. There are other combinations of A_2, A_4 and higher-order terms that can yield the similar good match too. It is highly likely that the presently observed ejection delay may primarily arise from the field distortion due to the holes drilled on the two end-cap electrodes [20].[3] However, since a complete map of the electric field inside this trap is not yet known, the number $A_4/A_2 = -3\%$ is supplied here only as a reference for the imperfections of the device used under our current experimental conditions.

3.3. Ejection delay due to buffer gas damping

Use of He buffer gas at a pressure of 1 mTorr has been a common practice in radio-frequency ion trap mass spectrometry for small molecules [4]. The practice takes advantage of the collisional cooling and focusing effect, which has been known [21] to enhance both the mass resolution and detection sensitivity of QITMS with the ion trap operated in an axial instability mode. Whetten [23] has shown in the early 1970s that introduction of buffer gas into a quadrupole ion trap would expand its stability diagram and shift the point of ejection significantly away from $q_{\text{eject}} = 0.908$. Such an effect can be dramatic for a trap operated at atmospheric pressure, where a value with $q_{\text{eject}} > 2$ results for microparticles [15]. Illustrated in Fig. 5b is the effect of damping on particle motion, obtained by computer simulation using Eq. (5) in this study. It is demonstrated therein that collisions of the particle with background He atoms of $b = 0.001$ can significantly reduce the amplitudes of its secular motions. However, a comparison of the particle motions in Fig. 5(a and b) indicates that damping of the particle by He in the mTorr range would not significantly alter the point of ejection ($q_{\text{eject}} \approx 0.908$) on the stability diagram for an ideal ion trap (see also Fig. 6a).

The above statement is no longer valid for a nonideal ion trap with a negative octopole component. Fig. 6b depicts the results of simulation for the damped motions after addition of an octopole term (−3%) to the modified Mathieu equation (Eq. (5)). Given with a reasonable initial position [$z(0) = 0.1$ mm] and velocity [$\dot{z}(0) = 0$ mm/s], significant differences in q_{eject} are found among the three cases, $b = 0$, 0.001 and 0.005. Compared to that of the ideal ion trap in Fig. 6a, there clearly exists an amplification of the delayed ejection in Fig. 6b. One may comprehend the amplification of this delay from Fig. 7(d and e) that the mass-selective scan for a nonideal ion trap with $A_4/A_2 < 0$ may achieve a larger deviation in q_{eject} from that of the ideal trap due to the presence of nonlinear electric fields. These deviations are, hence, more sensitive to the pressure of the buffer gas in the trap.

While the aerodynamic drag has an effect of causing additional ejection delays, the existence of buffer gas is essential (and even crucial) to the establishment of a stable ejection point, q_{eject}. This is particularly true for a trap operated in the AF region. For instance, it has been empirically found during the course of this simulation that, in the absence of buffer gas, the q_{eject} value may vary sensitively with the initial position and velocity of the particle in the trap.[4] Only with an increase of the damping constant up to $b = 0.005$ can the simulated q_{eject} value stabilize and become insensitive to the initial conditions.

The dependence of q_{eject} on b, if critical, may raise serious problems. Dahneke [25] has shown in an elaborate analysis that the b constant is a sensitive function of particle shape (either spherical or nonspherical). It suggests that the q_{eject} value of a nonideal ion trap (such as ours) may vary not only with the composition but also with the shape of the particles (with the same m/z) investigated. This is clearly not a desired feature when utilizing the ion trap as a mass spectrometer. To make a practical use of the audio-frequency ion trap mass spectrometer, efforts to minimize the content of the nonlinear fields in the trap are needed. This, fortunately, can be accomplished by adding a positive octopole term to compensate the superimposed negative octopole. A common solution to this problem is to symmetrically stretch the end-cap distance

[3] A calculation showed that the q_{eject} value would increase about 1% because of the presence of two 3 mm end-cap holes [28].

[4] Similar observations for small molecules have been reported in [18,19].

by about 11% on each side, as that have been experimentally demonstrated by Cooks and co-workers [20] and exploited by commercial QITMS [26]. Wang and co-workers [18] have theoretically predicted that stretching the end-cap electrode distance by $\Delta_z = +0.08$ mm would bring in an octopole term of the measure of $A_4/A_2 \approx +2\%$. This is about the right size of the modification that we need to do for our trap. It is expected that, with the field properly corrected by artificial superposition of positive high-order components, an m/z accuracy approaching 0.1% can be established after careful calibration of such an AF ion trap mass spectrometer.

4. Conclusion

Two conclusions have been reached from the present studies:

1. We have successfully developed a method to calibrate an audio-frequency quadrupole ion trap mass spectrometer, which can effectively cover the mass-to-charge range of 10^6 to 10^{10} by varying the trap driving frequency. The merit of this method is that it utilizes the ion trap itself as an electrodynamic balance, by which the mass-to-charge ratios of single trapped particles can be precisely determined. These single particles subsequently serve as calibrants for such mass spectrometers. For a trap having an axially stretched geometry with dimensions (r_0 and z_0) precise to within 0.01 mm, an m/z accuracy of the order of 10^{-3} is attainable.
2. We have determined the point of ejection for the AF ion trap mass spectrometer used in the present measurement to be $q_{\text{eject}} = 0.949 \pm 0.004$. The value, varying only slightly with the trap driving frequency over the range of $\Omega/2\pi =$ 200–600 Hz, is larger than 0.908 by a significant measure. It clearly indicates a delay in particle ejection. Revealed by computer simulations, the delay is predominantly resulted from the existence of multipole components (likely −3% of the octopole with respect to the basic quadrupole) of the fields in the trap due to device imperfections. These imperfections include truncation of the hyperbolic electrodes, holes drilled on the electrode assemblies, machining inaccuracy, as well as misalignments of the ring with respect to the two end-cap electrodes.

Acknowledgements

We thank the Academia Sinica and the National Science Council (NSC 90-2113-M-001-043) of Taiwan for financial support of this work.

References

[1] W. Paul, H. Steinwedel, US Patent 2,939,952 (1960); W. Paul, Rev. Mod. Phys. 62 (1990) 531.
[2] R.E. March, R.J. Hughes, Quadrupole Storage Mass Spectrometer, Wiley, New York, 1989.
[3] R.E. March, J.F.J. Todd (Eds.), Practical Aspects of Ion Trap Mass Spectrometry, Vol. 1, CRC Press, Boca Raton, 1995.
[4] J.N. Louris, R.G. Cooks, J.E.P. Syka, P.E. Kelley, G.C. Stafford Jr., J.F.J. Todd, Anal. Chem. 59 (1987) 1677.
[5] R.E. Kaiser Jr., R.G. Cooks, G.C. Stafford Jr., J.E.P. Syka, P.H. Hemberger, Int. J. Mass Spectrom. Ion Processes 106 (1991) 79.
[6] U.P. Schlunegger, M. Stoekli, R.M. Caprioli, Rapid Commun. Mass Spectrom. 13 (1999) 1792.
[7] N.L. Kelleher, M.W. Senko, M.M. Siegel, F.W. McLafferty, J. Am. Soc. Mass Spectrom. 8 (1997) 380.
[8] A.A. Rostom, C.V. Robinson, J. Am. Chem. Soc. 121 (1999) 4718; M.A. Tito, K. Tars, K. Valegard, J. Hajdu, C.V. Robinson, J. Am. Chem. Soc. 122 (2000) 3550.
[9] S.D. Fuerstenau, W.H. Benner, Rapid Commun. Mass Spectrom. 9 (1995) 1528; S.D. Fuerstenau, W.H. Benner, J.J. Thomas, C. Brugidou, B. Bothner, G. Siuzdak, Angew. Chem. Int. Ed. 40 (2001) 541.
[10] Y. Cai, W.-P. Peng, S.-J. Kuo, Y.T. Lee, H.-C. Chang, Anal. Chem. 74 (2002) 232.
[11] R.F. Wuerker, H. Shelton, R.V. Langmuir, J. Appl. Phys. 30 (1959) 342.
[12] E.J. Davis, Aerosol Sci. Tech. 26 (1997) 212.
[13] E.J. Davis, A.K. Ray, J. Colloid Interface Sci. 75 (1980) 566.
[14] M.A. Philip, F. Gelbard, S. Arnold, J. Colloid Interface Sci. 91 (1983) 507.
[15] H. Winter, H.W. Ortjohann, Am. J. Phys. 59 (1991) 807.
[16] G. Hars, Z. Tass, J. Appl. Phys. 77 (1995) 4245.
[17] S. Schlemmer, J. Illemann, S. Wellert, D. Gerlich, J. Appl. Phys. 90 (2001) 5410.

[18] Y. Wang, J. Franzen, Int. J. Mass Spectrom. Ion Processes 112 (1992) 167;
Y. Wang, J. Franzen, K.P. Wanczek, Int. J. Mass Spectrom. Ion Processes 124 (1993) 125;
J. Franzen, Int. J. Mass Spectrom. Ion Processes 125 (1993) 165;
Y. Wang, J. Franzen, Int. J. Mass Spectrom. Ion Processes 132 (1994) 155.
[19] M. Sudakov, Int. J. Mass Spectrom. 206 (2001) 27.
[20] J.M. Wells, W.R. Plass, G.E. Patterson, Z. Ouyang, E.R. Badman, R.G. Cooks, Anal. Chem. 71 (1999) 3405;
J.M. Wells, W.R. Plass, R.G. Cooks, Anal. Chem. 72 (2000) 2677.
[21] R.E. March, Int. J. Mass Spectrom. 200 (2000) 285.
[22] W.E. Moerner, Science 265 (1994) 46.
[23] N.R. Whetten, J. Vac. Sci. Technol. 11 (1974) 515.
[24] T. Hasegawa, K. Uehara, Appl. Phys. B 61 (1995) 159.
[25] B.E. Dahneke, Aerosol Sci. 4 (1973) 147.
[26] J.E.P. Syka, in: R.E. March, J.F.J. Todd (Eds.), Practical Aspects of Ion Trap Mass Spectrometry, Vol. 1, CRC Press, Boca Raton, 1995 (Chapter 4).
[27] A. Müller, Ann. Phys. 7 (1960) 6.
[28] Y. Cai, PhD thesis, Wuhan Institute of Physics and Mathematics, Chinese Academy of Sciences, Wuhan, China, 1998.